



Eidgenössische Technische Hochschule Zürich
Swiss Federal Institute of Technology Zurich



Jeremias Schmidli

Numerical Energy Analysis of PV Modules as Adaptive Building Shading Systems

Master Thesis

ITA – Architecture and Building Systems
Swiss Federal Institute of Technology (ETH) Zurich

Examiner: Prof. Dr. Arno Schlueter
Supervisor: Prageeth Jayathissa

Zurich, May 11, 2016

Abstract

Numerical optimization of the adaptive solar facade (ASF)

Contents

1	Introduction	1
1.1	Motivation and Literature Review	1
1.2	Problem Statement	2
1.3	Objectives of Research	2
1.4	Thesis Outline	3
2	Methodology	4
2.1	Simulation Tool Selection	4
2.1.1	Building Energy Simulation	4
2.1.2	Radiation Simulation	5
2.1.3	Photovoltaic Simulation	5
2.2	Combined Evaluation	6
2.3	Simulation Framework	6
2.4	Case Study	6
3	Results	9
3.1	Building Energy Analysis	9
3.2	Radiation and PV Analysis	11
3.2.1	Grid Convergence	11
3.2.2	Comparison of Sun Tracking to Optimized Solution	12
3.3	Combined Evaluation	13
3.3.1	Influence of Actuation	16
3.3.2	Orientation Analysis	17
3.3.3	Sensitivity Analysis	17
3.3.4	Potential of Individual Actuation	18
4	Discussion	19
5	Conclusion	20
6	Outlook	21
A	Appendix A	22

CONTENTS

iii

Bibliography

23

Chapter 1

Introduction

1.1 Motivation and Literature Review

Buildings are at the heart of society and currently account for 32% of global final energy consumption and 19% of energy related greenhouse gas emissions [1]. Nevertheless, the building sector has a 50-90% emission reduction potential using existing technologies [1]. Within this strategy, building integrated photovoltaics (BIPV) have the potential of providing a substantial segment of a building's energy needs [2]. Even the photovoltaic (PV) industry has identified BIPV as one of the four key factors for the future success of PV [3].

Dynamic building envelopes have gained interest in recent years because they can save energy by controlling direct and indirect radiation into the building, while still responding to the desires of the user [4]. This mediation of solar insolation offers a reduction in heating / cooling loads and an improvement of daylight distribution [5]. Interestingly, the mechanics that actuate dynamic envelopes couples seamlessly with the mechanics required for facade integrated PV solar tracking. Further literature on dynamic building envelopes includes [6], where current building performance simulations of adaptive facades are reviewed and the lack of adaptability in building simulation tools is addressed. Single axis dynamic shading has been evaluated in [7], emphasizing the importance of numerical evaluations in facade design decisions.

Previous BIPV research analyses electricity production and building energy demand for static BIPV shading systems [8–15]. The performance of fixed PV shading devices in dependence of different angles is analysed for cooling and electrical performance in [8] with a simplified PV electricity model. That work is extended in [9] to include different building orientations. In [10] the efficiency of fixed PV-shading devices is analysed, suggesting indices for comparison. [11] concludes that fixed surrounding PV shading devices are most efficient. The same authors assess different PV simulation

models in [12] and are able to show that extended electrical modelling is needed for complex PV geometry. [13] also includes visual comfort and finds brise-soleil systems to perform best. A first approach on assessing building energy demand with dynamic shading in combination with estimated PV electricity production is given in [15].

PV electricity production of shading devices has been evaluated for fixed angles in [16], where different BIPV facade geometries are analysed, finding horizontal louvers to perform best. In [17] a in-depth analysis of dynamic shading modules was evaluated for various design parameters with solar tracking.

This thesis expands on the work in [15] and [17] by analysing dynamic PV shading systems, while also taking into account mutual shading amongst modules and its effect on PV electricity generation. With this approach it is possible to reduce efficiency degradation due to partial shading of PV modules [17].

The work presented in this thesis is applied in the context of the Adaptive Solar Facade (ASF) project [18]. The ASF is a lightweight PV shading system composed of CIGS panels, that can be easily installed on any surface of new or existing buildings. This thesis will present a methodology of simulating an ASF while simultaneously calculating the energy demand of the office space behind the facade.

1.2 Problem Statement

Previous research has evaluated adaptive shading systems and building integrated photovoltaics, combined evaluations - however - could not be found in existing literature. Even though there already are prototypes of the adaptive solar facade - with new ones to be built soon - a comprehensive way to numerically analyse the energy demand combined with the electricity production is missing. A parametric model to analyse PV modules as adaptive solar shading systems needs to be developed in order to optimize the control strategy of said prototypes. Optimum configurations are yet to be found and the corresponding energy benefits must be evaluated. Finally, the potential of PV modules as adaptive building shading systems needs to be quantized in more detail, in order to asses the hypothesis of the energy benefits from the general concept.

1.3 Objectives of Research

Based on the problem statement, the objectives are to

- Develop a modelling framework to simulate the energetic performance of adaptive photovoltaic envelopes
- Find the best configurations to minimize the net building energy demand
- Assess effects of the building orientation, system parameters, location and simulation strategies
- Suggest factors that must be taken into account to find the optimum control strategy

1.4 Thesis Outline

Chapter 2 introduces the methodology used within this thesis and describes the approaches taken for building simulation, radiation and PV analysis as well as the combination of the two separate simulations. In chapter 3, the results for the building simulation and the electricity production are presented and different influences are shown. Chapter 4 then discusses the results and the influences they have on decision making for both further research and design optimization. The work is summarized and concludes in chapter 5 and an outlook for further research is given in chapter 6.

Chapter 2

Methodology

This chapter describes the methodology used to find the optimum configurations of the ASF. An evaluation of the tools that were selected and how they are combined to create a modelling framework is given, and details of the simulation methodology are described.

2.1 Simulation Tool Selection

To study the electricity generation and building energy consumption, a 3D geometry of the room and solar facade is built using the Rhinoceros software [19], and its parametric modelling plugin Grasshopper [20]. Rhinoceros is a state of the art computer-aided design (CAD) software, which can be used to generate complex geometries, such as the ASF. Combined with Grasshopper, which provides a visual programming language with a wide range of add-ons, it is particularly suited for simulations that are evaluating geometric structures. The simulation part can then be split up into three parts, namely *building energy simulations*, *radiation simulations* and *photo-voltaic simulations*. In the following the corresponding tools are described.

2.1.1 Building Energy Simulation

There are various building energy analysis engines, such as EnergyPlus [21] or TRNSYS [22]. As EnergyPlus is open source, widely used, and well documented, it was chosen as the building simulation engine for all simulations within this thesis. There are various ways of connecting to EnergyPlus. Within this thesis, mainly DIVA [23] and Honeybee [24] were evaluated. While Honeybee provides a large range of settings and adaptability, DIVA is kept very basic. However, the EnergyPlus analysis with honeybee is running significantly slower than with DIVA. Therefore, and for its simplicity, DIVA was chosen to connect Grasshopper with EnergyPlus. In EnergyPlus, the geometric solar facade is interpreted as an external shading system. Simulations are performed for a whole year at fixed angle positions, outputting

hourly values of energy use for heating, cooling and lighting. Optimum positions can then be found by comparing the electricity demand during every hour for all combinations.

2.1.2 Radiation Simulation

A solar radiance simulation is run using Ladybug [24], which is another grasshopper plugin and is developed by the same people as Honeybee. It includes various components to process weather data and calculate radiation on surfaces based on an automatically generated or a predefined mesh. Ladybug uses Radiance [25] to determine the incident insolation on the solar facade. This approach enables the calculation of solar irradiance on the modules with high spatial resolution including the effect of module mutual shading as seen in Figure 2.1. The radiation is analysed for cumulative monthly hours for the whole year.

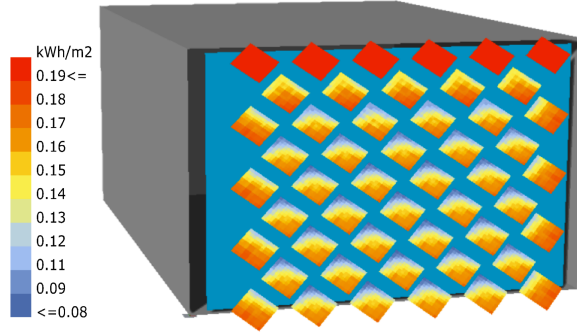


Figure 2.1: A simulation result showing module insolation from 11:00-12:00 on the 16 June for the used weather file and a specific module orientation.

2.1.3 Photovoltaic Simulation

The electrical model of the PV cells builds up on the methodology presented in [17] which is using the standard equivalent circuit model to calculate sub-cell I-V curves with a single diode, one series and one shunt resistance [26]. For the work in [17], the PV simulation was implemented with MATLAB. For this work, the MATLAB code was adjusted to match the new radiation simulations and then translated to python, in which the rest of the framework is written (details in section 2.3). PV electricity production is calculated based on a reference module. The model includes temperature dependency and irradiation dependency. The temperature is estimated as suggested in [27] with the following equation:

$$T_{cell} = T_{air} + \left(\frac{T_{cell}^0 - T_{air}^0}{S^0} \right) S_{cell} \quad (2.1)$$

where T_{cell} is the temperature of each grid point on the module, T_{air} is the ambient temperature, T_{cell}^0 is the temperature of the cell at reference insolation $S^0 = 800 \frac{W}{m^2}$ and reference air temperature $T_{air}^0 = 20^\circ C$, and S_{cell} is the insolation of each gridpoint in $\frac{W}{m^2}$. The value of T_{cell}^0 was estimated using thermal images of the solar facade and typical values given in [27].

2.2 Combined Evaluation

To combine the results of the building energy and the pv analysis, the building energy results were cumulatively combined to correspond to the pv analysis format. With this, the net energy usage of the room including the PV electricity production of the ASF can be given for monthly hours as described in equation 2.2.

2.3 Simulation Framework

In general the approach needs to solve the following optimization problem:

The following optimization problem has to be solved for PV modules as adaptive building shading systems:

$$\text{minimize}(C + H + L - PV) \quad (2.2)$$

Where C is the electricity needed for cooling, H is the electricity used for heating, L is the lighting power demand and PV represents the electricity production. Furthermore, different parameters must be evaluated to assess the effects of building orientation, possibilities and limits of current simulation tools, as well as various control strategy approaches.

Building energy simulations are achieved by using DIVA, whereas a radiation analysis is done with LadyBug, both within Grasshopper for Rhino. The results are then fed into a python script, which calculates the electricity production based on the radiation results and the surrounding temperature and post processes the information to calculate energy demand and optimum configurations. A corresponding workflow can be seen in Figure 2.2.

2.4 Case Study

The case study is done for a room and facade representing the prototype of the ASF at the house of natural resources (HONR) [18]. The solar facade consists of 400mm CIGS square panels that can rotate in two degrees of

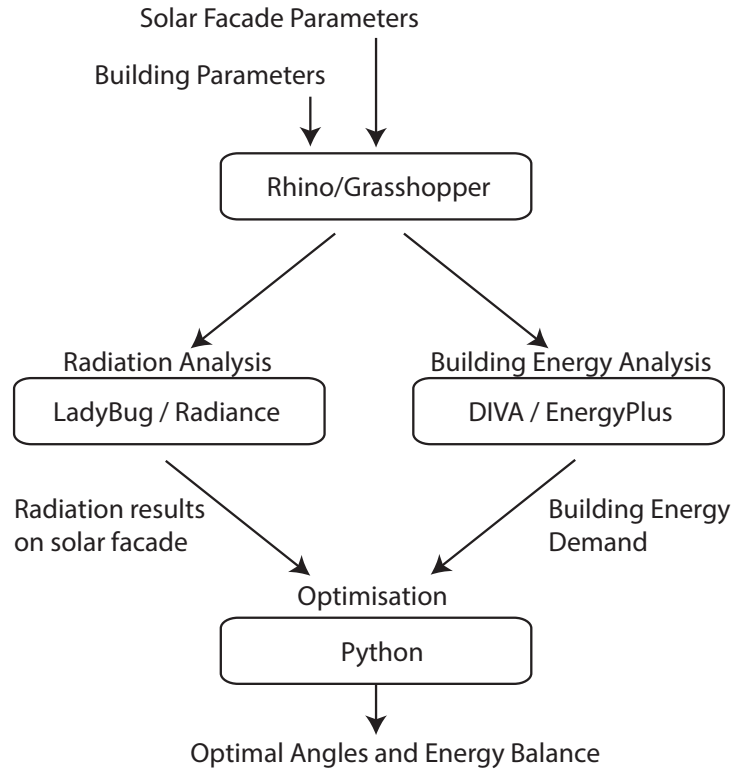


Figure 2.2: Work flow of the simulation framework

freedom. On the horizontal axis, the panels can move from 0° (closed) to 90° (open), whereas in the vertical axis, they can move from 45° to -45° .

The office environment is heated with a heatpump with an average COP of 4 and cooled with an average COP of 3. When required, the electric lighting consumption is 11.7 W/m^2 .

Simulations are run for different angle combinations, with a weather file for Kloten, Switzerland. The base case for the simulations consists of 25 angle combinations (five azimuth and 5 altitude angles), evaluated for averaged days of every month. The base-case scenario is then compared to control strategies where the angles are fixed or follow sun tracking and the sensitivity of various parameters, such as building orientation and COP. A corresponding picture of the prototype installed at the HONR, can be seen in figure 2.3.



Figure 2.3: Prototype of the adaptive solar facade on the house of natural resources

Chapter 3

Results

Optimum angles and their corresponding electricity use were found for the building energy simulation for all hours of the year. For the radiation and PV evaluations, a grid-convergence study was performed and results of an optimizing angle strategy was compared to sun-tracking. The combined simulations could then be evaluated to find the most efficient overall combinations and the sensitivities of various parameters on the system performance was found.

3.1 Building Energy Analysis

The optimal configurations of the ASF can be visualised using carpet-plots. For a classical building analysis this was done for every hour of the year. Figures 3.1 and 3.2 show the optimizing altitude and azimuth angles for heating, cooling, lighting and total building energy demand. In figure 3.1, darker colours represent closed positions, whereas brighter colours correspond to open positions. To optimize heating and lighting, open positions (corresponding to large altitude angles) are favourable, cooling is optimized by using closed positions (corresponding to small altitude angles). The overall optimized solutions follow the corresponding patterns at the hours of importance. The azimuth angles in figure 3.2 correspond to the deviation from the facade normal. For a south facing facade, this means an angle with a positive sign represents the panels facing towards south-east (bright colours), whereas negative angles represent the panels facing towards south-west (dark colours). It can be seen that for heating and lighting, the facade takes positions that let the sun in, whereas for cooling the facade follows a sun-tracking pattern which prevents radiation to enter the room.

Figure 3.3 depicts the corresponding energy demand of the building for the whole year corresponding to the optimum positions presented in figures 3.1 and 3.2. It can be seen that the heating heating is most needed during the winter and in the morning, whereas cooling is mainly apparent in

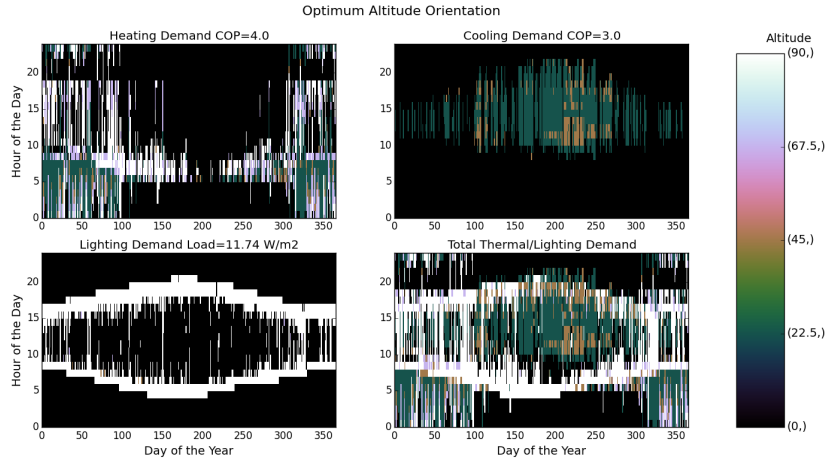


Figure 3.1: Carpet plots detailing the optimal altitude angles to minimise the (a) heating demand, (b) cooling demand, (c) lighting demand, and (d) total building energy demand. Darker colours represent closed positions, whereas brighter colors correspond to open positions. To optimize heating and lighting, open positions are favorable, cooling is optimized by using closed positions.

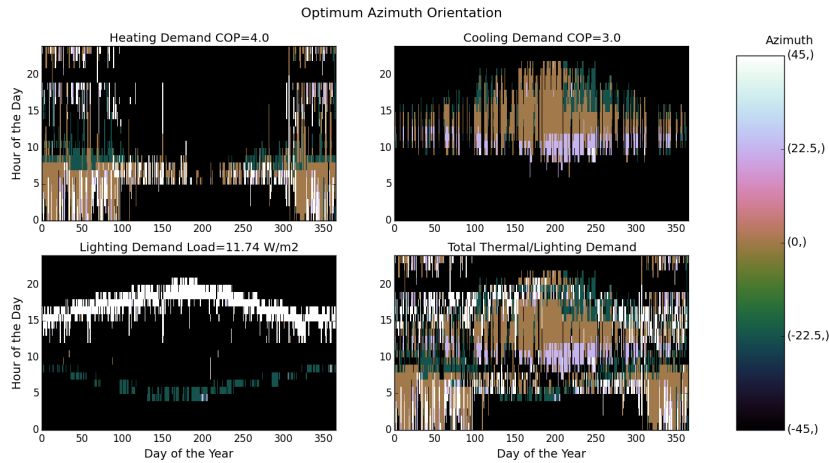


Figure 3.2: Carpet plots detailing the optimal azimuth angles to minimise the (a) heating demand, (b) cooling demand, (c) lighting demand, and (d) total building energy demand. Cooling is minimized by blocking the sun, whereas lighting and heating is minimized by opening the facade to let the insolation in.

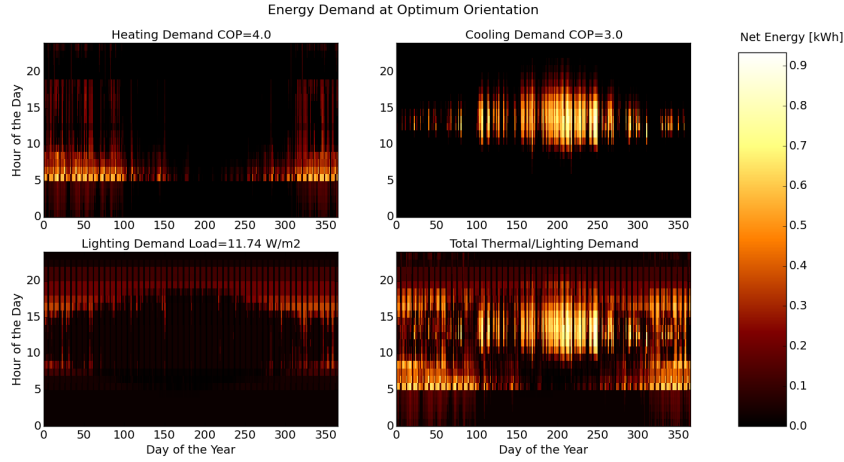


Figure 3.3: Carpet plots detailing the net energy consumption. Each square represents the total energy consumption for that specific hour of the entire month. Red colours detail the energy demand, while blue colours detail the energy supply.

summer afternoons. Lighting on the other hand is most important in the evenings and at times where there is not much sun. In the combined plot, this behavior be seen clearly as well, the main overlaps of different building energy consumptions take place during winter between heating and lighting in the morning and in the evening, and between cooling and lighting during summer evenings.

3.2 Radiation and PV Analysis

To evaluate the performance of the radiation simulation, a grid-convergence study was performed and the optimum grid size for further simulations was found. The radiation results could then be used to calculate the PV electricity production, enabling the finding of optimum angles to maximize PV electricity production. The corresponding energy output was finally compared to a control strategy using solar tracking.

3.2.1 Grid Convergence

With a larger grid-size, results are less accurate. In order to study this effect, a grid convergence study was conducted. Figure 3.4 shows the grid size dependency of the total radiation on the asf. The colors in the first two plots on the upper left represent the hours of the day. One can see in the second plot - where the radiation is normalized by a division with

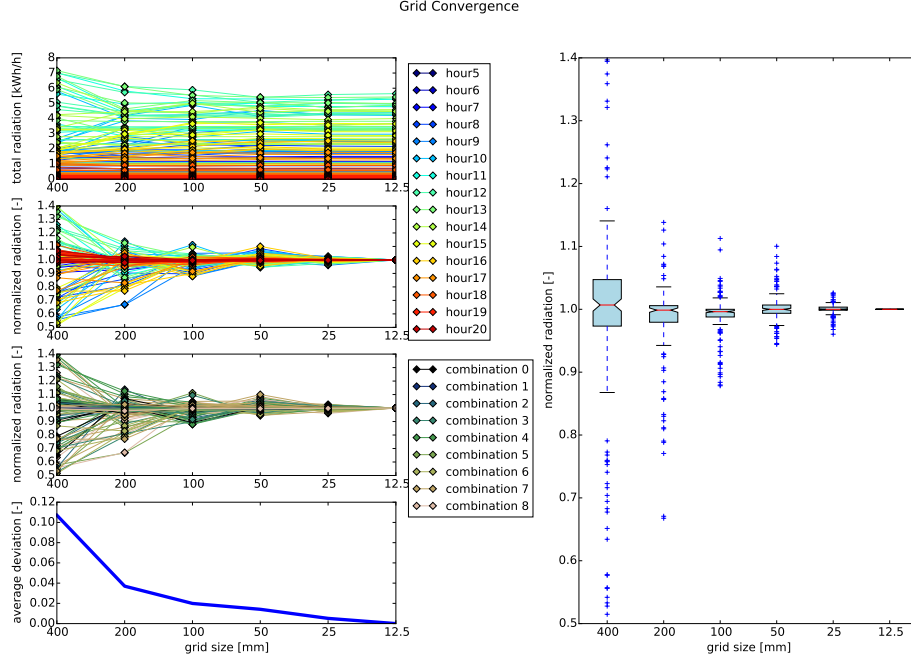


Figure 3.4: Grid convergence evaluation

the radiation for a grid-size of 12.5 mm - that the results are significantly more accurate for morning and evening hours. This is caused by increased self-shading at midday hours. The colours in the third plot on the left show the dependency on different combinations. No clear pattern could be found here. Finally the average deviation is depicted in the fourth plot on the left and a box-plot with all deviations is shown on the right. It can be seen that a smaller grid-size leads to larger deviations. While for a grid-size of 400 mm the average deviation is over 10%, the deviation goes down to below 1% for a grid size of 25 mm. 25 mm was therefore taken as the grid-size of all simulations, as it gives accurate results, while still being computationally feasible.

3.2.2 Comparison of Sun Tracking to Optimized Solution

In order to evaluate the optimum configuration for PV production, simulations using sun-tracking were compared to simulations evaluating 49 different combinations (i.e. 7 different azimuth and altitude angles). Figure 3.5 shows the radiation on the panels in the first plot, also comparing it to the maximum radiation. The second plot shows the PV electricity production for the two different control strategies, whereas the third plot compares the

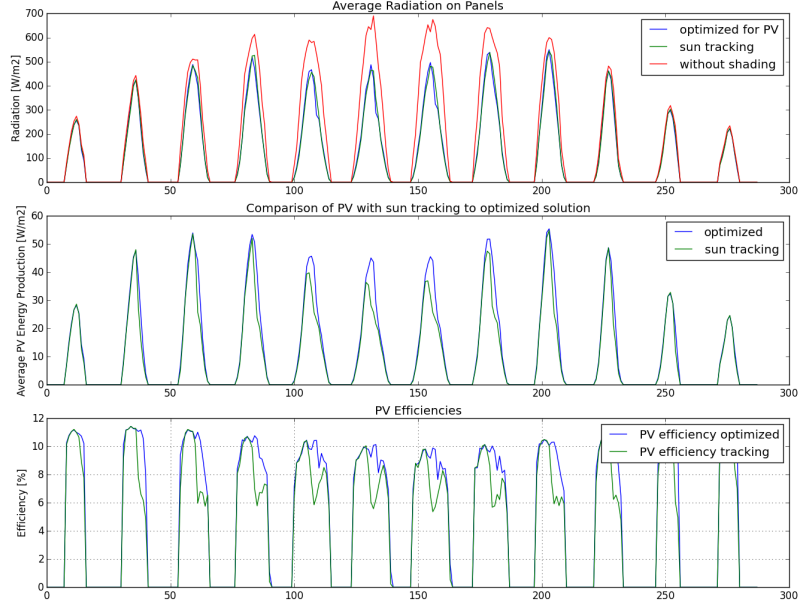


Figure 3.5: Comparison of optimized solution to sun-tracking. a) average radiation on panels compared to radiation without shading b) PV electricity production comparison c) efficiency comparison

corresponding efficiencies. It can be seen that while the radiation on the panels is pretty similar for both sun tracking and the optimized solution, the PV electricity production of the optimized solution is significantly higher than the sun-tracking solution in the afternoon hours. This is caused by the layout of the PV panels, longitudinal shading causes high power losses [17], thus the optimized solution decreases the longitudinal shading compared to sun-tracking.

3.3 Combined Evaluation

By combining results for building energy simulations and PV electricity production, the overall optimum configurations can be found. Figures 3.6 and 3.7 detail carpet-plots of the facade optimised to maximise PV generation, and minimise heating, cooling and lighting demands independently. Similarly to the building energy carpet plots in section 3.1, it can be seen that open configurations (light coloured) are chosen to minimise the building heating demands during the winter months and early mornings of spring

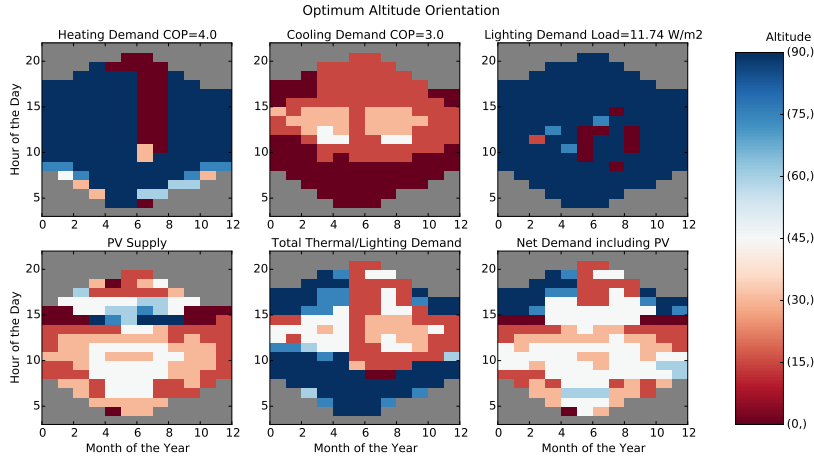


Figure 3.6: Carpet plots detailing the optimal altitude configuration to minimise the (a) heating demand, (b) cooling demand, (c) lighting demand, and (d) maximise irradiance on PV panels. Each configuration is represented by an angle of orientation around the x-axis (Altitude) and y-axis (Azimuth) as seen in the legend. Figure (e) details the combinations for optimum building thermal management without PV production. (f) also includes the PV production

and autumn. Likewise, closed configurations (dark colours) are the preferred solutions to minimise the cooling demand during the summer months. For lighting control, open positions are the optimum at all times, while the optimum altitude angles is almost exclusively at 90° , the azimuth angles are at -45° in the morning and at 45° in the afternoon. The PV optimisation tends to choose angles that are not that extreme, corresponding to the minimization of longitudinal shading as described in section 3.2.2. When the four optimisation cases are combined to achieve the configurations for total energy minimisation, it can be seen that there is a conflict in the summer evenings between minimising lighting and cooling demands. Likewise, we also see a conflict between heating and PV production during the winter months. The overall energy optimization including PV electricity production shows a strong tendency to follow the optimal PV production pattern. This, however changes if the building system becomes more inefficient. Less efficient heating for example, would result in configurations optimised for heating overpowering those of PV electricity generation.

Figure 3.8 shows the net energy use at these optimum angles. It is interesting to see how the combination of electricity generation and adaptive shading can compensate for the entire energy use during sunlit hours.

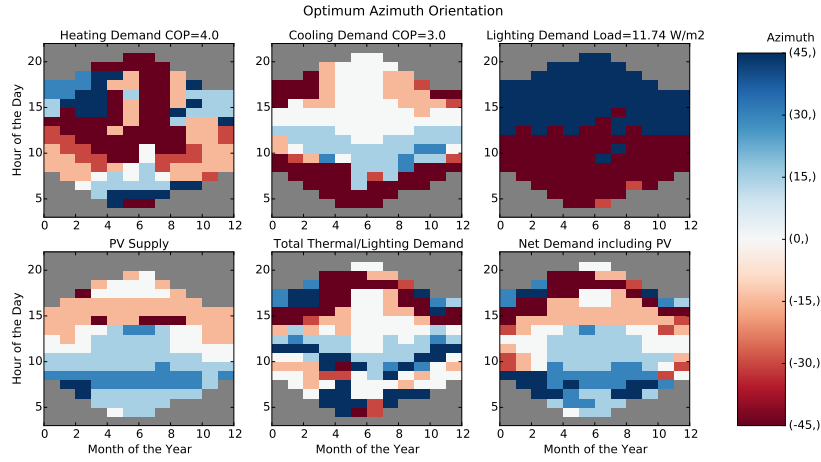


Figure 3.7: Carpet plots detailing the optimal azimuth configuration to minimise the (a) heating demand, (b) cooling demand, (c) lighting demand, and (d) maximise irradiance on PV panels. Each configuration is represented by an angle of orientation around the x-axis (Altitude) and y-axis (Azimuth) as seen in the legend. Figure (e) details the combinations for optimum building thermal management without PV production. (f) also includes the PV production

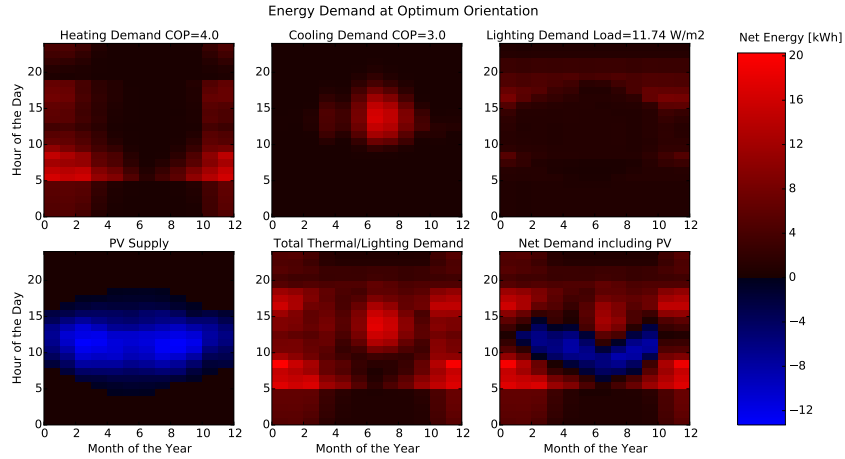


Figure 3.8: Carpet plots detailing the net energy consumption. Each square represents the total energy consumption for that specific hour of the entire month. Red colours detail the energy demand, while blue colours detail the energy supply.

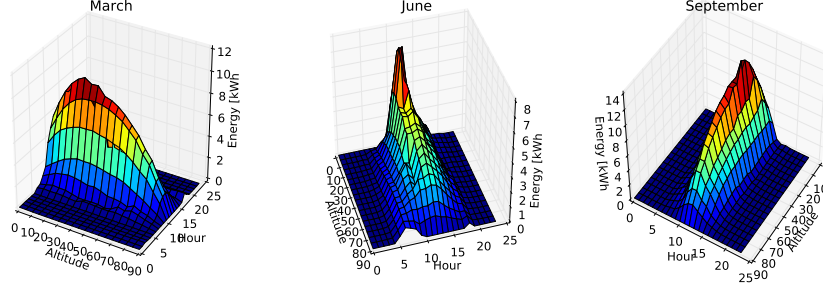


Figure 3.9: Energy benefits of the altitude actuation for the months of March, June and September. Each plot displays one cumulative day in hourly resolution. The x-axis represents the hour of the day, the y-axis represents the altitude angles, and the z-axis represents the energy benefit of the actuation, i.e. the difference in energy usage between the evaluated angle and the angle that yields the worst overall energy usage for each hour.

3.3.1 Influence of Actuation

In order to evaluate the influence of the actuation, three dimensional plots can be used to display all possible configurations and their corresponding energy benefit. In figure 3.9, the energy benefits of the altitude actuation can be seen for the months of March, June and September. Each plot displays one cumulative day in hourly resolution. The x-axis represents the hour of the day, the y-axis represents the altitude angles, and the z-axis represents the energy benefit of the actuation, i.e. the difference in energy usage between the evaluated angle and the angle that yields the worst overall energy usage for each hour. It can be seen that the energy benefit is by far the largest around noon. Furthermore, positions that are rather closed tend to have the highest influence for the said mid-day hours. Open positions normally yield the worst benefits, except for some early morning or evening hours, where heating and lighting become important. This overall behaviour corresponds well to the results depicted in figure 3.6, and shows why the angles that yield the optimum total energy, generally match the angles that optimize cooling and PV electricity production. A further interesting observation that can be made from this figure is the non continuous curves for midday hours, at an altitude angle of around 30° , the energy benefit reduces over proportionally. This is caused by the PV electricity production, larger angles will increase longitudinal shading and therefore over proportionally reduce the energy yield.

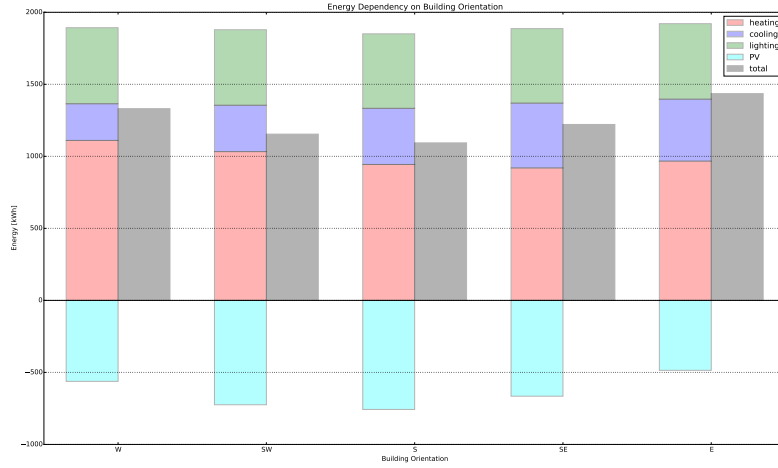


Figure 3.10: Energy demand in dependence of building orientation. South facing facades perform best.

3.3.2 Orientation Analysis

Evaluations of the facade for different building orientations were done with the basecase of 5 azimuth and 5 altitude angles. Non surprisingly, the south facing facade produces the most electricity and has therefore the lowest net energy as can be seen in figure 3.10. It was found that the PV apertures should be oriented parallel to the upper left edge for facades that are west or south-west oriented, whereas they should be oriented parallel to the upper right edge for east or south-east oriented facades. This is caused by the shading patterns, longitudinal shading needs to be prevented as described in section 3.2.2. An east facing facade uses less heating compared to a west facing facade, as heating is most important during morning hours. For similar reasoning the east facing facade needs more cooling energy than the west facing facade, because the room heats up in the morning. Interestingly, PV production is higher for the west facing facade than for the east facing facade. The cause for this is probably because of conflicts in optimizing cooling and PV electricity production at the same time, as cooling is more dominant for the east facing facade.

3.3.3 Sensitivity Analysis

A sensitivity analysis was done for heating COP, cooling COP, lighting load, average PV efficiency, building orientation, infiltration rate and combination variations for the time period of one year. The results are shown in figure

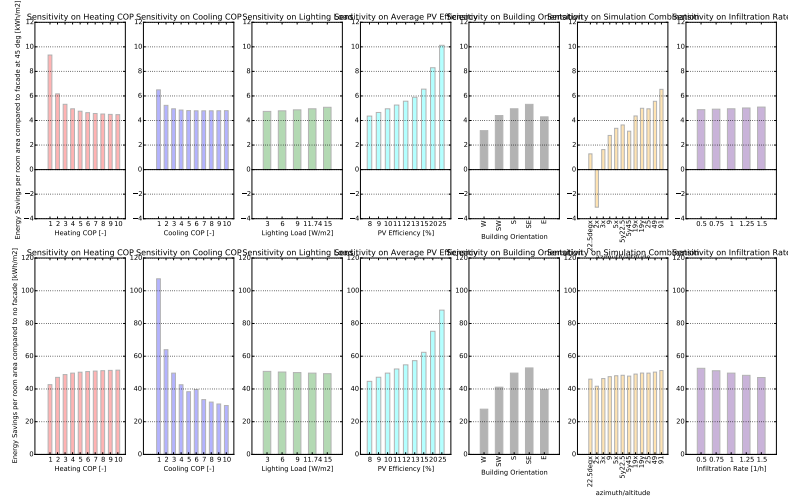


Figure 3.11: Sensitivity analysis of energy savings during one year. From left to right, sensitivities on heating COP, cooling COP, lighting load, average PV efficiency, building orientation, combination variations and infiltration rate. Top row shows the energy savings compared to a fixed solar facade at a 45° altitude angle, the bottom row shows the energy savings compared to a room without shading or PV modules.

3.11. The top row shows the energy savings per square meter of room area compared to a fixed solar facade at an angle of 45° , whereas the bottom row shows the energy savings compared to a building without any PV modules or shading devices.

3.3.4 Potential of Individual Actuation

Individual actuation of the panels is one of the key advantages of the ASF that have to be closely evaluated. In order to quantize the potential of individual actuation, evaluations were performed by splitting the ASF into clusters. Due to computational limitations, especially on the radiation part, a simplified geometry was used for the evaluation, using only 10 panels in 4 rows, rather than the 50 panels of the reference case. Furthermore only the months of March, June, September and December were evaluated.

Chapter 4

Discussion

Building energy demand could be minimized, while the PV electricity production could be maximized. Generally it can be said that for heating and lighting, open positions are favorable whereas closed positions are needed for cooling and PV electricity production. As the PV electricity production is strongly dependent on the self-shading of the facade, the positions that optimize PV electricity production do not match a sun-tracking pattern, as longitudinal shading has to be minimized. Therefore angles need to be chosen, that would be less efficient for a single module without self shading, but are minimizing the longitudinal self shading on the panels.

Chapter 5

Conclusion

In this thesis, a simulation methodology to evaluate a dynamic photovoltaic shading system is presented, combining both electricity generation, and the energy demand of the building. It is then coupled with a post processing python script to determine the optimum system configuration for control. The methodology can be applied to evaluate different PV system geometries, building systems, building typologies and climates.

The dynamic PV integrated shading system has clear advantages to a static system as it can adapt itself to the external environmental conditions. This enables it to orientate itself to the most energy efficient position. The optimum orientation however, strongly depends on the general efficiency of the building. Decreasing the efficiency of the heating, cooling or lighting systems will give higher preference for configurations optimised for building thermal management through adaptive shading, than for PV electricity production.

This work ultimately presents a methodology for the planning and optimisation of sophisticated adaptive BIPV systems. Future work will use this methodology to determine the environments and building typologies that could benefit from adaptive BIPV systems.

Chapter 6

Outlook

While the results of this thesis are promising, further research must be done on many aspects. Optimization algorithms must be found to determine the best state of the system with individual actuation while taking into account all influences. The optimization algorithms must be included into the control of a real system, so that it can be at the optimum position at all times. Influences of user satisfaction and comfort has to be evaluated as well and must ultimately be included in the optimum control methods. Furthermore, the PV panels should be connected into strings for the evaluation and the influence of bypass-diodes should be included. In order to evaluate the building performance in more detail, the methodology needs to be changed to calculate building energy demand for single hours, taking into account the inertia of the system. Also the energy needed for the actuation of the panels should be modelled and included into the optimization, to determine whether the energy savings from the improved position are higher than the actuation energy needed to get to that position.

Furthermore, the electrical PV model should be enhanced to include the possibility of simulating different string connections of panels as well as the use of bypass diodes.

Appendix A

Appendix A

This is appendix A

Bibliography

- [1] Fifth assessment report, mitigation of climate change. *Intergovernmental Panel on Climate Change*, pages 674–738, 2014.
- [2] PR Defaix, WGJHM van Sark, E Worrell, and Erika de Visser. Technical potential for photovoltaics on buildings in the eu-27. *Solar Energy*, 86(9):2644–2653, 2012.
- [3] Marco Raugei and Paolo Frankl. Life cycle impacts and costs of photovoltaic systems: current state of the art and future outlooks. *Energy*, 34(3):392–399, 2009.
- [4] RCGM Loonen, M Trčka, Daniel Cóstola, and JLM Hensen. Climate adaptive building shells: State-of-the-art and future challenges. *Renewable and Sustainable Energy Reviews*, 25:483–493, 2013.
- [5] Dino Rossi, Zoltán Nagy, and Arno Schlueter. Adaptive distributed robotics for environmental performance, occupant comfort and architectural expression. *International Journal of Architectural Computing*, 10(3):341–360, 2012.
- [6] Roel C.G.M. Loonen, Fabio Favoino, Jan L.M. Hensen, and Mauro Overend. Review of current status, requirements and opportunities for building performance simulation of adaptive facades. *Journal of Building Performance Simulation*, 0(0):1–19, 0.
- [7] Martin Vraa Nielsen, Svend Svendsen, and Lotte Bjerregaard Jensen. Quantifying the potential of automated dynamic solar shading in office buildings through integrated simulations of energy and daylight. *Solar Energy*, 85(5):757–768, 2011.
- [8] L.L. Sun and H.X. Yang. Impacts of the shading-type building-integrated photovoltaic claddings on electricity generation and cooling load component through shaded windows. *Energy and Buildings*, 42(4):455 – 460, 2010.
- [9] Liangliang Sun, Lin Lu, and Hongxing Yang. Optimum design of shading-type building-integrated photovoltaic claddings with different

- surface azimuth angles. *Applied Energy*, 90(1):233 – 240, 2012. Energy Solutions for a Sustainable World, Special Issue of International Conference of Applied Energy, ICA2010, April 21-23, 2010, Singapore.
- [10] M. David, M. Donn, F. Garde, and A. Lenoir. Assessment of the thermal and visual efficiency of solar shades. *Building and Environment*, 46(7):1489 – 1496, 2011.
- [11] M Mandalaki, K Zervas, T Tsoutsos, and A Vazakas. Assessment of fixed shading devices with integrated pv for efficient energy use. *Solar Energy*, 86(9):2561–2575, 2012.
- [12] M. Mandalaki, S. Papantoniou, and T. Tsoutsos. Assessment of energy production from photovoltaic modules integrated in typical shading devices. *Sustainable Cities and Society*, 10:222 – 231, 2014.
- [13] M Mandalaki, S Papantoniou, and T Tsoutsos. Assessment of energy production from photovoltaic modules integrated in typical shading devices. *Sustainable Cities and Society*, 10:222–231, 2014.
- [14] Seung-Ho Yoo and Heinrich Manz. Available remodeling simulation for a bipv as a shading device. *Solar Energy Materials and Solar Cells*, 95(1):394–397, 2011.
- [15] Prageeth Jayathissa, Zoltan Nagy, Nicola Offedu, and Arno Schlueter. Numerical simulation of energy performance and construction of the adaptive solar facade. *Proceedings of the Advanced Building Skins*, 2:52–62, 2015.
- [16] Freitas Sara and et al. Maximizing the solar photovoltaic yield in different building facade layouts. *EU PVSEC (2015)*, 2015.
- [17] Johannes Hofer, Abel Groenewolt, Prageeth Jayathissa, Zoltan Nagy, and Arno Schlueter. Parametric analysis and systems design of dynamic photovoltaic shading modules. *EU PVSEC 2015 conference, Hamburg, Germany (paper in review)*.
- [18] Zoltan Nagy, Svetozarevic Bratislav, Prageeth Jayathissa, Moritz Begle, Johannes Hofer, Gearoid Lydon, Anja Willmann, and Arno Schlueter. The adaptive solar facade: From concept to prototypes. *under review*.
- [19] Rhinoceros v5, 2015.
- [20] Grasshopper - algorithmic modeling for rhino, 2015.
- [21] Drury B Crawley, Linda K Lawrie, Curtis O Pedersen, and Frederick C Winkelmann. Energy plus: energy simulation program. *ASHRAE journal*, 42(4):49–56, 2000.

- [22] University of Wisconsin-Madison. Solar Energy Laboratory and Sanford A Klein. *TRNSYS, a transient system simulation program*. Solar Energy Laboratary, University of Wisconsin-Madison, 1979.
- [23] Diva for rhino.
- [24] M Roudsari, Michelle Pak, and Adrian Smith. Ladybug: A parametric environmental plugin for grasshopper to help designers create an environmentally-conscious design. 2014.
- [25] Gregory J Ward. The radiance lighting simulation and rendering system. In *Proceedings of the 21st annual conference on Computer graphics and interactive techniques*, pages 459–472. ACM, 1994.
- [26] Andr   Mermoud and Thibault Lejeune. *Performance assessment of a simulation model for PV modules of any available technology*. Proceedings of the 25th European Photovoltaic Solar Energy Conference. WIP, M  nchen, 2010. ID: unige:38547.
- [27] R.G. Jr. Ross and M.I. Smokler. *Flat-Plate Solar Array Project: Final report: Volume 6, Engineering sciences and reliability*. Oct 1986.